

# Transformer Energization Studies with Uncertain Power System Configurations

M. Martínez-Duró, F.-X. Zgainski, B. Caillault

**Abstract**—This paper presents a method for studying transformer energization effects when the characteristics of the supplying power system are uncertain. “Supplying power system” stands for the transmission grid, the generation plants and the loads connected to the grid. The characteristics of this system are uncertain when a large number of configurations (grid topology, in-service generation plants, and connected loads) are possible but only several of them can be precisely characterized.

Moreover, the influence of the system parameters on the risk of temporary overvoltages is analyzed, and a method to find the minimum short-circuit power level beyond which the energization of a given transformer does not present any risk is presented.

**Keywords:** Transformer energization, Temporary overvoltages, Uncertainty, Monte Carlo, Power system transients, Power transformers, Power system modelling, Frequency dependent network equivalents, EMTP.

## I. INTRODUCTION

THE energization of transformers in power systems is generally performed without any adverse consequence. However, in certain situations, the transient currents and voltages generated at the energization can lead to several problems [1]. One of these problems is the generation of temporary overvoltages (TOV). The occurrence of TOV at the energization depends on the existence of low-frequency parallel-resonances (i. e., presenting maximum impedance values) in the supplying network, which may be excited by the harmonic components of the inrush currents [2].

As a general approach, the lower the resonance frequency and the higher the resonance impedance, the most likely TOV will be generated. If these TOV are high enough, the equipment (mainly the energized transformer itself) may be damaged.

This paper presents a real case where a 200 MVA 400/10 kV transformer must be energized. This transformer is connected to the 400 kV grid through a 580 m cable. An already energized but unloaded 64 MVA 400/7 kV transformer is connected to the same point through a 720 m cable. See Fig. 1.

At the point where the transformers are connected, the grid

is poorly meshed. This means that the transformers are fed by long overhead lines (OHL) and as consequence the resonance frequencies may be low. Moreover, as the grid is poorly meshed, the loss of one these OHL (whether unforeseen or planned) could worsen the problem. Therefore, the goal of the study is to determine if the energizing of the 200 MVA transformer at that point of the grid may involve a risk of equipment damage.

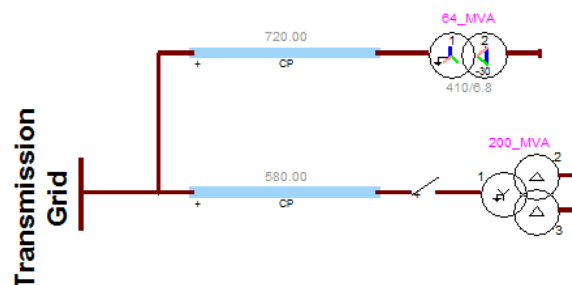


Fig. 1: System to be studied (transmission grid, cables, circuit breaker, power transformers)

However, the supplying system configuration is not completely defined: on the one hand, many grid topologies are possible depending on the unavailable OHLs; on the other, the power plants and loads connected to the grid can also vary. Furthermore, during normal operation, the utility (i. e., the power generating facility owner) does not know the actual system configuration, the only available information about the system is the short-circuit power at the connection point (provided by the Transmission System Operator, TSO). Thus the problem to be addressed is: what is the minimum short-circuit power of the grid for the transformer to be safely energized?

## II. GENERAL RELATIONSHIP BETWEEN $S_{sc}$ AND $Z(f)$

The occurrence of TOV at the transformer energization depends on the supplying system frequency response, i. e., its impedance-versus-frequency characteristic,  $Z(f)$ . This characteristic depends on the grid topology and the connected power plants and loads.

However, as the only information on the grid that will be available on a daily basis is its short-circuit power ( $S_{sc}$ ), the relationship between  $S_{sc}$  and  $Z(f)$  needs to be investigated. For this the simple generic system shown in Fig. 2 is considered. It is made of  $N_{gen}$  generators each of them supplying  $N_{lines}$  parallel OHL of  $l_{lines}$  length, all of them meeting at the *target point*. All the generators have the same impedance and all the lines have the same per length characteristics.  $N_{gen}$  represents the system size, i. e., the total electric power generation of the

M. Martínez Duró is with Electricité de France, R&D Division, Clamart, France ([manuel.martinez@edf.fr](mailto:manuel.martinez@edf.fr)).

F.-X. Zgainski and B. Caillault are with Electricité de France, DTG Division, Grenoble, France ([francois.zgainski@edf.fr](mailto:francois.zgainski@edf.fr), [bruno.caillault@edf.fr](mailto:bruno.caillault@edf.fr)).

system.  $N_{lines}$  represents the degree of meshing of the grid. Of course, this system is extremely simple, but it can provide general guidelines on the behaviour of real systems.

First of all, the short-circuit power at the target point is given by:

$$S_{sc} \cong \frac{U^2}{2\pi f_P} \cdot \frac{N_{gen}}{L_{gen} + \frac{l_{lines}}{N_{lines}} \cdot L_{line,km}} \quad (1)$$

Where  $f_P$  is the system power frequency (in our case, 50 Hz),  $U$  is the system voltage (400 kV),  $L_{gen}$  is the generator inductance, and  $L_{line,km}$  is the lines per-length inductance (all these values are constants). Notice that the loads are considered not to have any influence on the short-circuit power, as the load impedances are much higher than those of the generators and lines.



Fig. 2. Simple generic power system with  $N_{gen}=3$  and  $N_{lines}=3$

Expression (1) shows a simple but important fact: for a given system size (i. e., a given number of generators,  $N_{gen}$ ),  $S_{sc}$  depends on the ratio  $l_{lines}/N_{lines}$ . This means that the same short-circuit power  $S_{sc}$  can correspond to a grid which is very meshed and is made of long lines or to a grid that is less meshed but has shorter lines. This already suggests that there is no unique relationship between  $S_{sc}$  and  $Z(f)$ . This is going to be demonstrated hereafter.

Our main interest in  $Z(f)$  is the first parallel resonance, characterized by its frequency (resonance frequency) and its amplitude (resonance impedance).

For the moment, let's assume the system is unloaded. The circuit in Fig. 2 is a parallel composition of  $N_{gen}$  identical circuits, each of which can be simplified in an equivalent circuit consisting in a series RL in parallel with a C. For such a circuit, the resonance frequency can be approximated as [3]

$$f_{res} \cong \frac{1}{2\pi\sqrt{LC}}, \text{ if } R \ll \sqrt{L/C} \quad (2)$$

By applying expression (2) to the circuit in Fig 1 and using expression (1), the lowest resonance-frequency at the target point is given by:

$$f_{res} \cong K_1 \cdot \frac{S_{sc}}{N_{lines}} \cdot \sqrt{\frac{K_3}{K_2 - S_{sc} \cdot K_4}} \quad (3)$$

with

$$K_1 = \frac{1}{U \cdot \sqrt{\frac{2\pi \cdot N_{gen} \cdot C_{line,km}}{f_P}}}$$

$$K_2 = \frac{U^2}{2\pi f_P} \cdot N_{gen}$$

$$K_3 = L_{line,km}$$

$$K_4 = L_{gen}$$

where  $C_{line,km}$  is the lines per-length capacitance.

The expression (3) shows that, for a given system size, the resonance frequency at the target point varies almost linearly with the ratio  $S_{sc}/N_{lines}$ . This means that the first resonance frequency of the system depends both on the short-circuit power *and* the degree of meshing of the grid. There is no unique relationship between  $f_{res}$  and  $S_{sc}$ : a higher short-circuit power does not imply that the resonance frequencies are higher: this is only true for a given degree of meshing. On another hand, for a given short-circuit power, more meshed grids have lower resonance frequencies. However, more meshed grids have lower impedance amplitudes, as this is going to be shown below.

Again, analyzing the circuit in Fig. 2 as a parallel RL//C circuit, it can be demonstrated that, *if the system is unloaded*, the resonance impedance, i. e., the impedance at the lowest resonance-frequency, is roughly proportional to the short-circuit power and inversely proportional to the square of the meshing of the grid:

$$Z_{res} = Z(f_{res}) \propto \frac{S_{sc}}{N_{lines}^2} \quad (\text{no load}) \quad (4)$$

On the one hand, the resonance impedance decreases with the square of the degree of meshing. On the other hand, for a given degree of meshing, the resonance impedance increases with the short-circuit power of the system.

Considering that the TOV are more likely to occur when the system resonance has low frequency and high amplitude, expressions (3) and (4) show that the variation of the short-circuit power or the degree of meshing have always two opposite effects: increasing the short-circuit power increases the resonance frequency but it also increases the resonance amplitude, whereas increasing the meshing decreases the resonance amplitude but also the frequency.

So far, the system was considered unloaded. However, both the frequency and the impedance of the resonance depend on the loads connected to the grid. Unfortunately, it seems impossible to derive an analytical expression of  $f_{res}$  and  $Z_{res}$  without oversimplifying the equivalent circuit. Therefore, in order to investigate the influence of the load on  $Z(f)$ , several frequency-domain simulations on the circuit in Fig. 2 for different values of the load have been performed. Three load spatial distributions were investigated: uniformly distributed over the length of all the lines, concentrated at the generators end, concentrated at the target point. The results of the

simulations show that the influence on the resonance frequency is small (it slightly increases with increasing load). On the contrary, the influence on the resonance impedance is very important. Although this influence depends on the load location, *the resonance impedance completely depends on the load level: the larger the load, the smaller the resonance impedance*. Thus, the expression (3) is suitable only when considering an unloaded system, for instance during a power restoration process after a blackout.

### III. SETTING $Z(f)$ UNCERTAINTIES FROM AVAILABLE SYSTEM DATA

As explained in section I, the power system supplying the transformer at the target point is not well defined, as both the grid topology and the generation/load level can change over the time as a result of many uncontrollable factors. Moreover, the goal of the study is to provide a short-circuit power level above which the energization of the transformer is safe, no matter the system conditions that lead to that short-circuit power level.

However, it has been shown that the short-circuit power is not enough to characterize the system frequency response, in particular the system resonances. For this reason, RTE, the French TSO, was requested to provide the  $Z(f)$  characteristic for several potential system configurations, depending on the lines in service and on the power generation units and loads connected to the grid. These characteristics are obtained by simulation in the frequency domain with a model of the whole French network.

Fig. 3 and Fig. 4 provide the direct and zero sequence impedance amplitude,  $Z_+(f)$  and  $Z_0(f)$ , at the system connection point for five system configurations. The corresponding phase curves were also provided but are not shown. For all of them, the system load is the same and kept at a low level in order to consider the most unfavourable network configuration.

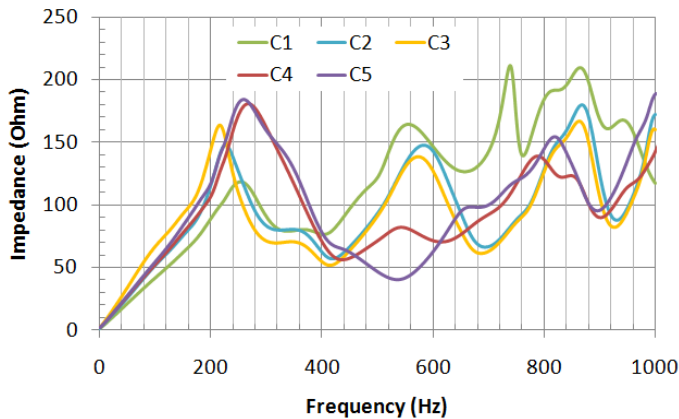


Fig. 3. Direct sequence impedance,  $Z_+(f)$ , at the system connection point for several grid configurations

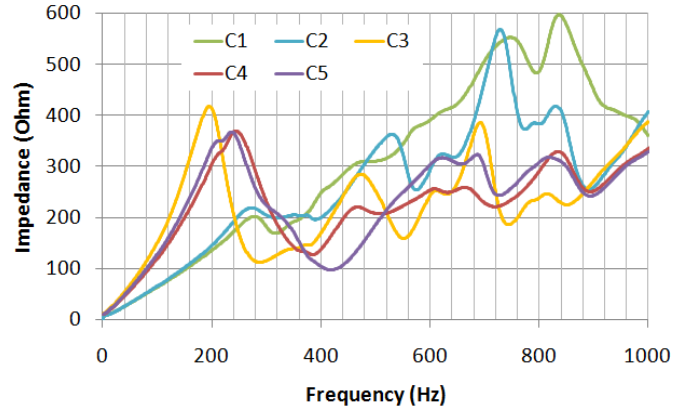


Fig. 4. Zero sequence impedance,  $Z_0(f)$ , at the system connection point for several grid configurations

The short-circuit power of each system configuration is given in Table I. Roughly, the  $S_{sc}$  varies between 3400 and 6000 MVA. Configurations 2, 4 and 5 show the fact that, as explained in the previous section, the frequency response of the system is not uniquely linked to the short-circuit power level: whereas configurations 4 and 5 have similar  $S_{sc}$  and  $Z(f)$ , configurations 2 and 4 (or 2 and 5) have similar  $S_{sc}$  but quite different  $Z(f)$ . As for the first resonance, the one that is more likely to be excited by the inrush currents, the maximum difference between these configurations having similar  $S_{sc}$  are (see Fig. 3 and Fig. 4) summarized in Table II. Roughly, the resonance frequency and impedance change by 12-25%, except for the zero sequence resonance impedance, which goes up to 65% difference.

All these figures are for a constant system load. In order to assess the impact of the load level, RTE provided complementary simulation results. These simulations corroborated our findings in the previous section, as the resonance amplitude is multiplied by 1.8 when the load is divided (uniformly all over the grid) by 2.

TABLE I  
SHORT-CIRCUIT POWER OF EACH SYSTEM CONFIGURATION

System configuration	$S_{sc}$ (MVA)
1	5940
2	4940
3	3420
4	4820
5	4870

TABLE II  
DIFFERENCES IN  $Z(f)$  BETWEEN CONFIGURATIONS 2 AND 4/5

Resonance frequency	Direct sequence	20%
	Zero sequence	12%
Resonance impedance	Direct sequence	25%
	Zero sequence	65%

Now, remember that the utility was requesting a minimal short-circuit power level for the transformer energization to be safe. Of course, the lower this minimal value of  $S_{sc}$ , the better. For this reason, it was decided that the simulation study would be performed by using configuration 3 as a reference, the configuration with the lowest  $S_{sc}$  (3420 MVA). Thus,  $Z_{ref}(f) = Z_{C3}(f)$ . However, in order to account for the potential variations of  $Z(f)$  for the same  $S_{sc}$ , at least the following uncertainties should be considered on  $Z_{ref}(f)$ :

- The resonance frequencies can vary in a  $\pm 25\%$  range.
- The resonance impedances can vary in a  $[0,100]\%$  range.

These are the minimal uncertainty ranges to be accounted for. However, wider ranges will be considered as well in order to be more conservative.

#### IV. SUPPLYING SYSTEM MODELLING

The supplying system is made of the transmission grid and the connected loads and generators. The only available information on this system is the frequency response,  $Z_{ref}(f)$ , and the associated uncertainties put forward in section III. Two kinds of Frequency Dependent Network Equivalent (FDNE) are used to model the supplying system: accurate and simplified.

##### A. Accurate FDNE by Vector Fitting

First, the Vector Fitting technique is presented; afterwards, the method to take into account the uncertainties on  $Z(f)$ .

##### 1) Space-State Model of $Z(f)$ by Vector Fitting

In the accurate approach, a Norton equivalent of the system is implemented where the impedance matches exactly the frequency response  $Z(f)$  provided by the TSO (RTE). The power-frequency current source is set to match the short-circuit power  $S_{sc}$ . This equivalent is shown in Fig. 5, where the current source is three-phase and direct sequence and  $Z(f)$  is three-phase and thus represents self and mutual impedances.

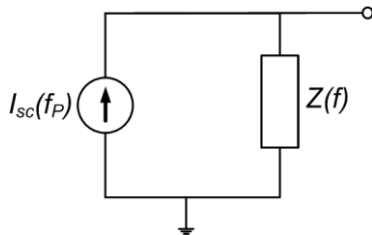


Fig. 5. Norton equivalent of the supplying system

The impedance block  $Z(f)$  is modelled by a state-space model. The matrices defining this model are calculated by using the public domain implementation of the vector fitting technique provided in [4]. The vector fitting technique (see [5] to [9]) approximates a linear frequency-dependent function  $y(s)$  by a rational function:

$$y(s) \cong \sum_{n=1}^N \frac{r_n}{s - a_n} + d + s \cdot e, \quad s = j \cdot 2\pi \cdot f$$

In this expression,  $a_n$ ,  $r_n$ ,  $d$  and  $e$  are the poles, the residues,

the constant and the linear terms, respectively. These parameters are calculated iteratively in order to fit a given sample  $y(f_i)$ ,  $i=1..m$ . When fitting the elements of an admittance matrix,  $Y(s)$ , each of its elements is fitted independently except for the poles, which are assumed to be the same for all the elements.

The previous pole-residue model can then be formulated as a state-space model of the form [10] (capital letters are matrices):

$$Y(s) = C \cdot (s \cdot I - A)^{-1} \cdot B + D + s \cdot E$$

This state-space model can be directly included in EMTP-RV, where it can be used both in frequency and time domain simulations.

##### 2) Accounting for uncertainties on $Z(f)$

In our case, the input matrices  $Y(f_i)$  are calculated from the sequence impedances  $Z_+(f_i)$  and  $Z_0(f_i)$  of the system. These impedances are calculated from those provided by the TSO for the system configuration no. 3,  $Z_{ref}(f)$ , and by taking into account the uncertainties on the resonance frequencies and impedances. For this, a number of modified frequency responses,  $Z_{mod}(f)$ , are built in this way (the modifications are applied both to direct and zero sequence impedances):

- The amplitude of  $Z_{ref}(f)$  is multiplied by 3.
- The curve  $Z_{ref}(f)$  is frequency-shifted (both in amplitude and phase) in the range  $[-115, +115]$  Hz by steps of 1 Hz. As the first resonance frequency of  $Z_{ref}(f)$  is 215 Hz, this allows to cover the case where the resonance is located at the first power frequency (50 Hz) harmonic, i. e. 100 Hz.

This provides 231 potential frequency responses of the supplying system,  $Z_{mod}(f)$ , which are modelled in the time domain by state-space models calculated by Vector Fitting in the range 0-1000 Hz (1 Hz step) with 50 poles.

The modification technique needs to be further specified. In fact, the goal is to increase the resonance impedance and shift the resonance frequencies in order to account for other system configurations having different frequency responses but the same short-circuit power as the reference,  $Z_{ref}(f)$ . The  $Z_{ref}(f)$  at power frequency and below shouldn't be altered, because this part of  $Z_{ref}(f)$  determines the short-circuit power. Therefore, the modification of  $Z_{ref}(f)$  is applied this way:

- For  $f \leq 60$  Hz,  $Z_{ref}(f)$  is not modified.
- For  $f \geq 190$  Hz,  $Z_{ref}(f)$  is modified as previously explained. For instance, for the  $Z_{mod}(f)$  corresponding to a 50 Hz shift, the amplitude of the curve  $Z_{ref}(f)$  is multiplied by 3 (both in direct and zero sequence) and 50 Hz are subtracted to the  $Z_{ref}(f)$  frequencies (for both amplitude and phase curves, for direct and zero sequence).
- For  $60 \text{ Hz} \leq f \leq 190 \text{ Hz}$ , the amplitude and frequency modification is linearly introduced, i. e., it is proportional to  $(f-60)/(190-60)$ . This avoids jumps in  $Z_{mod}(f)$ .

As an example, the Fig. 6 shows the direct sequence amplitude of  $Z_{ref}(f)$  and the modified  $Z_{mod}(f)$  for -115 Hz, 0 Hz

and +115 Hz shifts.

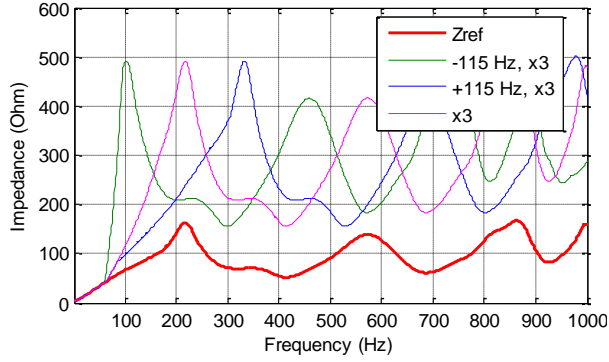


Fig. 6.  $Z_{ref}(f)$  and  $Z_{mod}(f)$  for -115 Hz, 0 Hz, and +115 Hz shifts and an amplitude factor 3 (direct sequence amplitude)

This is the method by which the 231  $Z_{mod}(f)$  curves are calculated, which are then used as the input data for the vector fitting algorithm. However, the more the initial curve  $Z_{ref}(f)$  has been altered, the worse the fitting of the resulting  $Z_{mod}(f)$ . This is normal: as it has been obtained by simulation,  $Z_{ref}(f)$  is physically consistent (i. e., stable, causal and passive), but the  $Z_{mod}(f)$  computed by alteration of  $Z_{ref}(f)$  are not, especially for important alterations. The reason is that the amplitude and phase angle of a physically consistent system are uniquely linked, and our alterations of  $Z_{ref}(f)$  break this link. Then, as the vector fitting algorithm (with the passivity enforcement technique implemented in [4]) enforces the output to be physically consistent, the response of the equivalents can be quite different from the input  $Z_{mod}(f)$ . Of course, this problem worsens as the difference between  $Z_{mod}(f)$  and  $Z_{ref}(f)$  increases. (This problem could be overcome by fitting only the amplitude of  $Z_{mod}(f)$ , but this is not implemented in the present version of the VF routines).

The problem is illustrated in Fig. 7 showing the direct sequence impedance of the state-space network equivalents built for frequency shifts of -115 Hz, 0 Hz, and +115 Hz and an impedance factor of 3. The result for the equivalent built from the original  $Z_{ref}(f)$  is also shown in red colour. These curves have been obtained by a frequency scan in EMT-P-RV. The responses of all the other network equivalents are intermediate cases. By comparing Fig. 6 and Fig. 7, it can be seen that the frequency shift is fairly correct, but not the amplitude, which is too low: the more important the frequency shift to the left, the worse the amplitude fitting.

However, in the  $\pm 25\%$  frequency-shift range, the resonance amplitude of the network equivalents is always higher than twice the resonance amplitude in  $Z_{ref}(f)$ . As a consequence, the network equivalents comply with the requirements stated in section III. In conclusion, the 231 network equivalents built according to the previous methodology will be used.

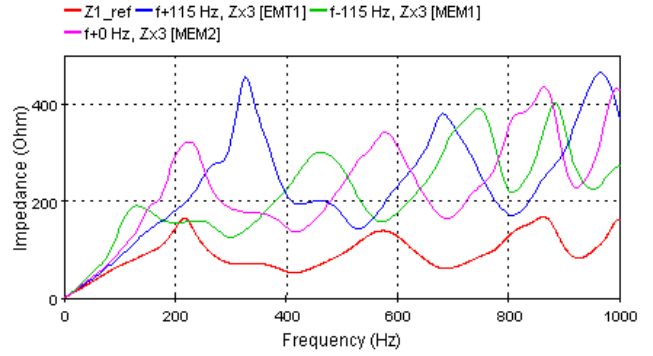


Fig. 7. Direct sequence impedance of the network equivalents for a frequency shift of -115 Hz, 0 Hz, and +115 Hz. Original  $Z_{ref}(f)$  shown in red color.

### B. Simplified IEC 71-4 equivalent

In addition to the accurate FDNE by Vector Fitting, the power supply equivalent suggested by IEC 71-4 for TOV ([11] §7.4.1) has been used too as a simpler alternative. See Fig. 8. This model represents the short-circuit impedance and one single resonance (both in direct and zero sequence). The drawback of this model is that only the frequency and the amplitude of the resonance can be controlled, not the global shape of  $Z(f)$  which is much flatter than the real one. As an illustration, the Fig. 9 compares  $Z_{ref}(f)$  and the corresponding model  $Z(f)$ .

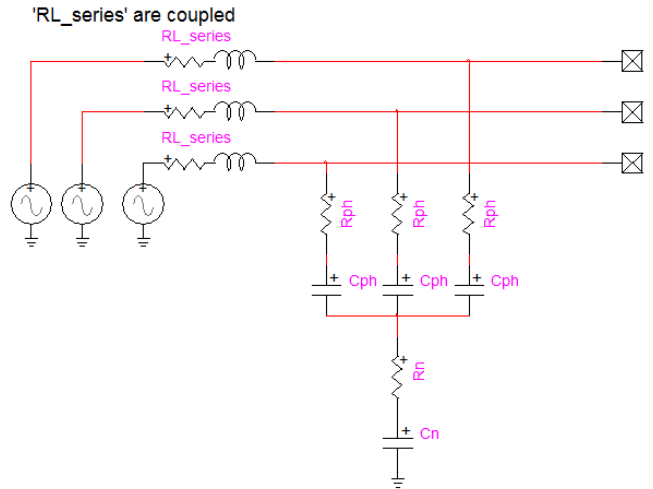


Fig. 8. IEC 71-4 power supply equivalent for TOV ([11] §7.4.1)

The series impedances are derived from the short-circuit impedance (direct and zero sequence) of the system, i. e., the value of  $Z(f)$  at  $f=f_r=50\text{Hz}$ . The values of the parallel capacitances  $C_{ph}$  and  $C_n$  are computed according to the direct and zero sequence resonance frequencies. The parallel damping resistances  $R_{ph}$  and  $R_n$  are computed using an optimisation algorithm that minimizes the distance between the maximum of the sought  $Z(f)$  curve and the maximum of the  $Z(f)$  curve computed with the model.

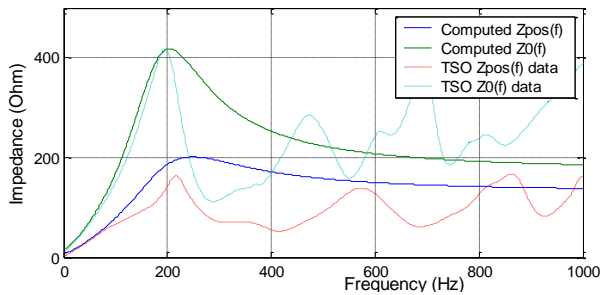


Fig. 9: Direct and zero sequence impedances: comparison between model  $Z(f)$  and  $Z_{ref}(f)$

## V. OTHER SYSTEM COMPONENTS MODELLING

Besides the supplying system, the network components that need to be modelled are the transformers, the cables, and the circuit breaker. It is important to model the already energized 64 MVA transformer because a sympathetic interaction phenomenon may occur and increase the duration of the transient currents and voltages.

### A. Transformers

The transformers are modelled in a standard way. The energized transformer is three-phase shell-type 200 MVA 400/10 kV YNdd11. The short-circuit behaviour between the three windings (1 HV, 2 LV) is modelled by an inductance matrix (as in BCTRAN) accounting for the leakage flux. The load losses are modelled by series resistances at the winding terminals. The nonlinear behaviour of the core is modelled by three nonlinear inductors and three parallel linear resistances. These branches are connected to the LV windings and are calculated iteratively in order to match the no-load tests, which provide the RMS current for 90%, 100%, and 110% excitation. After the point obtained from the 110% excitation test, the flux/current curve of the nonlinear inductors is extended in order to match the air-core inductance provided by the manufacturer, 1.4 H seen from the HV side. As the LV windings are delta connected, the zero sequence behaviour of the core can be neglected.

The already energized transformer is core-type 64 MVA 400/7 kV YNd. It is modelled in the same manner.

### B. Cables

Each cable link is modelled by a PI circuit.

### C. Circuit-breaker

The circuit-breaker is modelled as an ideal switch.

## VI. UNCERTAINTIES MODELLING

Several parameters are known with some uncertainty that must be taken into account [12][13]. One can distinguish *epistemic parameters*, those whose uncertainty is due to a limited knowledge of the system, and *aleatory parameters*, those whose uncertainty is due to the intrinsic random behaviour of the physical phenomena. The transformer air-core reactance and the supplying system  $Z(f)$  are epistemic parameters; the transformer residual flux and the circuit-

breaker closing times are aleatory. These uncertainties need to be statistically characterized and a suitable stochastic simulation technique must be used to propagate them to the output.

### A. Target transformer residual fluxes

It is assumed that the target transformer was deenergized at unloaded condition. Therefore, the small no-load current was chopped by the circuit-breaker. In this case, assuming a symmetrical system, the phase transient fluxes after the deenergization form a  $120^\circ$  phase-shifted balanced symmetrical set (see experimental results in [14]). The final values of the fluxes, i. e. the residual fluxes, are unknown but they range between 0 and 80% of the flux at the rated transformer voltage.

Let  $\lambda_r$  be the flux at the rated voltage and  $\lambda_0$  and  $\theta$  two auxiliary variables representing the amplitude and the phase angle of the balanced symmetrical set of the residual fluxes. According to the preceding considerations,  $\lambda_0$  can take any value between 0 and  $0.8\lambda_r$  and  $\theta$  any value between 0 and  $360^\circ$ . In statistical terms,

$$\lambda_0 = 0.8\lambda_r U[0,1]$$

$$\theta = U[0, 360^\circ]$$

where  $U[a,b]$  represents a uniform distribution between  $a$  and  $b$ . The potential residual flux values in the three wounded legs of the transformer are then obtained from the values of  $\lambda_0$  and  $\theta$  as:

$$\lambda_k = \lambda_0 \cdot \cos(\theta + (k-1) \cdot 120^\circ), \quad k = 1 \dots 3$$

### B. Target transformer air-core reactance

The air-core reactance of the energized transformer, which is an important parameter [15], is provided by the manufacturer with 20% accuracy. Therefore, it is modeled by a uniform distribution centered at the provided value, 0.16 pu, and covering a  $\pm 20\%$  range. This is:  $L_{air-core} = U[0.13, 0.19]$  pu.

### C. Circuit-breaker closing times

The circuit-breaker closing times uncertainty is modelled by four random parameters: a *common order time*, the same for the three poles of the CB, and the random *offset time* of each pole due to the mechanical pole spread:  $t_{close,i} = t_{order} + t_{offset,i}$   $i=1..3$ . The common order time may take any value in the sine wave, thus following an uniform probability distribution over the power frequency period  $T$  (equal to 20 ms if  $f_p=50$  Hz). The offset time of each pole is considered to follow a Gaussian law whose mean is zero (the three poles tend to close simultaneously) and whose standard deviation ( $\sigma$ ) is calculated from the maximum pole span, MPS (i. e., the maximum delay between poles). The three  $t_{offset,i}$  follow the same Gaussian law  $N(0, \sigma)$ . As the interval  $\pm 3\sigma$  has 99.7% probability in a Gaussian distribution, the standard deviation may be calculated from this interval width as  $\sigma = MPS/6$ . A rather conservative 20 ms maximum delay between poles has been considered. For  $MPS=20$  ms,  $t_{order} = U[100, 120]$  ms,  $t_{offset,i} = N(0, 3.3)$  ms.

#### D. Supplying system $Z(f)$

The supplying system frequency response  $Z(f)$  uncertainty has been characterized in section III. The  $Z(f)$  to be used in the simulations is chosen according to a discrete uniform distribution  $k_Z = DU\{1..n\}$ , where  $n$  is the number of state-space network equivalents, i. e.,  $n=231$ .

#### E. Stochastic simulation: Monte Carlo method

Stochastic simulation techniques provide a way to compute the output variables probability distributions given the probability distributions of the input parameters. The best known one, the Monte Carlo method, will be used.

The Monte Carlo method estimates the output variable probability distribution by simulating a sufficient number of outputs corresponding to random samples of the uncertain parameters. This means that a large number of simulations will be run; for each simulation, the values of the parameters  $\lambda_0$ ,  $\theta$ ,  $L_{air-core}$ ,  $k_Z$ ,  $t_{order}$ ,  $t_{offset,i}$  ( $i=1..3$ ) will be a random sample of the corresponding distribution.

### VII. RESULTS

#### A. Monte Carlo Simulations with the Accurate FDNE Model

The simulations are performed with EMTP-RV coupled to MATLAB, in which the Monte Carlo algorithm is implemented.

The simulated time is 3 seconds.

As an illustration, the figures below provide the temporal waveform of the currents and voltages at the transformer terminals for one of the simulated cases. Fig. 10 shows the inrush current at the 200 MVA energized transformer. Fig. 11 shows that no significant overvoltage is generated (the voltage at the two transformers is identical). Fig. 12 shows that the 64 MVA transformer goes into saturation by sympathetic interaction.

In order to account for the uncertainties of the parameters, 3000 Monte Carlo simulations are performed. For each simulation, the maximum voltage at the two transformers (200 MVA and 64 MVA), phase-to-ground ('V') and phase-to-phase ('U') is stored.

The Fig. 13 shows the cumulative distribution functions (CDF) for these four voltages. These distributions demonstrate that no dangerous overvoltage is generated at the energization of the 200 MVA transformer, the maximum voltage value being always less than 1.15 pu. It can be concluded that the short-circuit power of the reference system configuration (no. 3), 3420 MVA, can be used as a minimal value beyond which the energization does not generate overvoltages.

Note that, as none of the simulations exceeded the overvoltage capability of the transformers, the so-called *rule of 3* [16] states that the real risk is between 0% and 0.1% ( $3/N$ ,  $N=3000$ ) with 95% confidence.

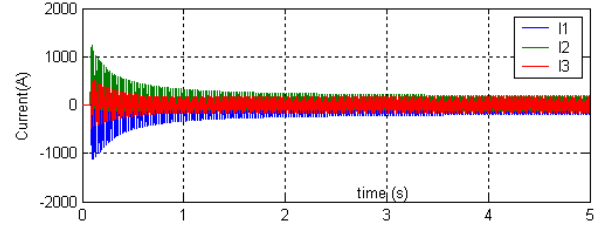


Fig. 10. Inrush currents at the 200 MVA transformer

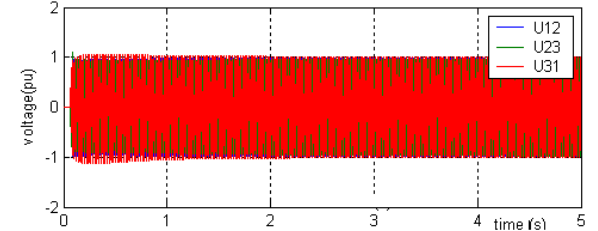


Fig. 11. Voltage at the 200 MVA transformer terminals

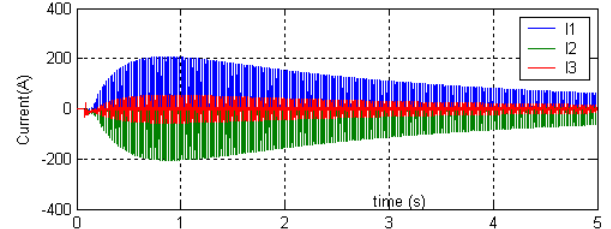


Fig. 12. Sympathetic inrush currents at the 64 MVA transformer

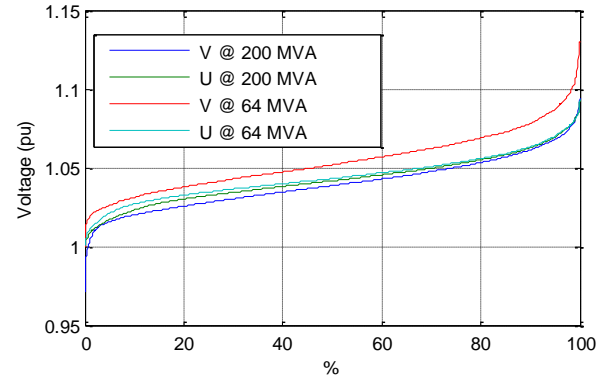


Fig. 13. Overvoltage CDFs (phase-to-ground, 'V'; phase-to-phase, 'U')

#### B. Extreme Case Simulations with the Simple System Model

The simple system model has been used to simulate an extreme  $Z(f)$  case: the resonance frequency is set to  $f_{res}=150$  Hz and the resonance amplitude is set to four times the first resonance amplitude of  $Z_{ref}(f)$ . For comparison purposes, another simple model is built with  $f_{res}$  and  $Z(f_{res})$  equal to those of the first resonance of  $Z_{ref}(f)$  (see Fig. 9). The simulation results are shown in Fig. 14 and Fig. 15 respectively. Each figure shows the envelopes of the absolute values of the voltages at the terminals of the 200 MVA transformer for different sets of values of the uncertain parameters  $\lambda_0$ ,  $\theta$ ,  $L_{air-core}$ ,  $t_{order}$ ,  $t_{offset,i}$ .

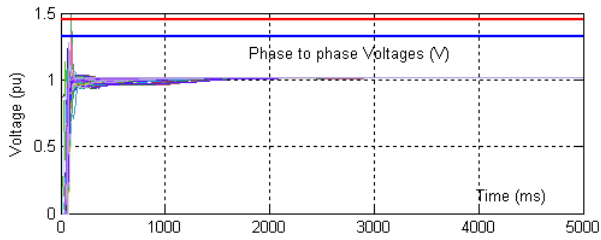


Fig. 14: Voltages with the simple model for  $f_{res}=215$  Hz and  $\max(Z(f))=\max(Z_{ref}(f))$

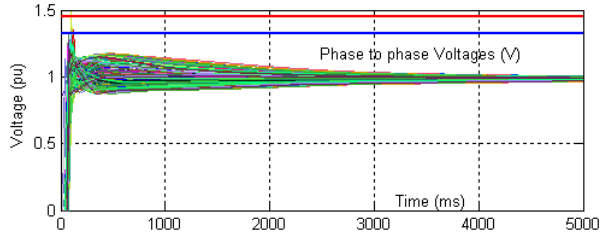


Fig. 15: Voltages with the simple model for  $f_{res}=150$  Hz and  $\max(Z(f))=4\max(Z_{ref}(f))$

In these two figures, the TOV are radically different. In the reference case, no significant TOV is generated. In the extreme case, they can reach the level of 700 kV (1.2 pu) approximately 0,5 seconds after the closing of the CB. However, the short-circuit power is the same in both cases.

### VIII. CONCLUSIONS

The goal of the study was to evaluate the risk of temporary overvoltages (TOV) when energizing a 400 kV 200 MVA transformer, close to which a 64 MVA transformer is already energized (but unloaded). As these transformers are located at a point where the transmission grid is poorly meshed, TOV could be generated if the inrush currents excited a parallel resonance of the grid. In addition, contingent events as line outage can reduce the meshing and thus increase the risk of overvoltage.

The main problem was that the frequency response of the supplying system was poorly defined: several  $Z(f)$  curves were provided by the TSO along with the associated  $S_{sc}$ , but other potential configurations of similar  $S_{sc}$  (corresponding to other grid topologies, and generation and load levels) needed to be considered as well. Moreover, the main objective was to define a minimal  $S_{sc}$  level beyond which the energization does not generate any dangerous temporary overvoltages.

To provide an answer to this problem, the relationship between  $Z(f)$  and  $S_{sc}$  was investigated. This investigation showed that, in general, knowing the short-circuit power of the system is not enough to assess the risk of TOV when energizing a power transformer. Indeed, the resonance frequency and amplitude of the system impedance are not uniquely linked to its short-circuit power level.

However, the investigation permitted to define uncertainties associated to the  $Z(f)$  provided by the TSO in order to account for other system configurations with similar  $S_{sc}$ . By Monte Carlo simulation taking into account these uncertainties and

those on the target transformer residual fluxes and air-core reactance, and on the CB closing times, it was determined that 3420 MVA can be used as an operational  $S_{sc}$  lower limit (although the minimal  $S_{sc}$  is probably smaller).

The method developed in this paper is general. It can be used in any other similar case where the characteristics of the supplying system are uncertain.

### IX. ACKNOWLEDGMENTS

The authors gratefully acknowledge the helpful contribution of Nicola Chiesa on the residual fluxes potential values, and that of Bjorn Gustavsen on the vector fitting technique. Thanks are also due to Yannick Vernay, from RTE, who performed the calculations of the supplying system impedance,  $Z_{Ci}(f)$ .

### X. REFERENCES

- [1] CIGRE WG C4.307, *Transformer Energization in Power Systems: A Study Guide*, to be published in 2013.
- [2] D. Povh, Schultz W, "Analysis of overvoltages caused by transformer magnetizing inrush current", IEEE Transactions on Power Apparatus and Systems, 1978, 97(4): 1355-1365.
- [3] C. L. Wadhwa, *Network Analysis & Synthesis*, 2nd Revised Edition, New Delhi, New Age International, 2006.
- [4] B. Gustavsen (ed.), *The Vector Fitting Web Site*, <http://www.energy.sintef.no/Produkt/VECTFIT/index.asp>
- [5] B. Gustavsen and A. Semlyen, "Rational approximation of frequency domain responses by Vector Fitting", IEEE Trans. Power Delivery, vol. 14, no. 3, pp. 1052-1061, July 1999.
- [6] B. Gustavsen, "Improving the pole relocating properties of vector fitting", IEEE Trans. Power Delivery, vol. 21, no. 3, pp. 1587-1592, July 2006.
- [7] D. Deschrijver, M. Mrozowski, T. Dhaene, and D. De Zutter, "Macromodeling of Multiport Systems Using a Fast Implementation of the Vector Fitting Method", IEEE Microwave and Wireless Components Letters, vol. 18, no. 6, pp. 383-385, June 2008.
- [8] A. Semlyen and B. Gustavsen, "A half-size singularity test matrix for fast and reliable passivity assessment of rational models", IEEE Trans. Power Delivery, vol. 24, no. 1, pp. 345-351, January 2009.
- [9] B. Gustavsen, "Fast passivity enforcement for pole-residue models by perturbation of residue matrix eigenvalues", IEEE Trans. Power Delivery, vol. 23, no. 4, pp. 2278-2285, October 2008.
- [10] B. Gustavsen, H.M.J. De Silva, "Inclusion of Rational Models in an Electromagnetic Transients Program – Y-Parameters, Z-Parameters, S-Parameters, Transfer Functions", accepted for publication in IEEE Transactions on Power Delivery.
- [11] IEC TR 60071-4:2004, "Insulation co-ordination – Part 4: Computational guide to insulation co-ordination and modelling of electrical networks".
- [12] M. Martínez-Duró and R. Denis, "Parameter uncertainty assessment in the calculation of the overvoltages due to transformer energization in resonant networks," in CIGRE Session, Paris, France, 2012.
- [13] F-X.Zgainski, B.Caillault and V-L.Renouard, "Validation of power plant transformers re-energization schemes in case of black-out by comparison between studies and fields tests measurements," in IPST07, Lyon, 2007.
- [14] N. Chiesa, A. Avendano, H. K. Høidalen, B. A. Mork, D. Ishchenko and A. P. Kunze, "On the ringdown transient of transformers," in IPST07, Lyon, 2007.
- [15] M. Martínez-Duró, "Damping Modelling in Transformer Energization Studies for System restoration: Some Standard Models Compared to Field Measurements", in *PowerTech 2009*, Bucarest, 2009.
- [16] J. Hanley and A. Lippman-Hand, "If nothing goes wrong, is everything all right? Interpreting zero numerators," JAMA, vol. 35, pp. 1743-1745, 1983.